

Atomic-matter-wave scanner

Hilmar Oberst,^{1,*} Shigenori Kasashima,¹ Victor I. Balykin,² and Fujio Shimizu¹¹*Institute for Laser Science, University of Electro-Communications, Chofu-shi, Tokyo 182-8585, Japan*²*Institute of Spectroscopy, Russian Academy of Science, Troitsk 142092, Moscow Region, Russian Federation*

(Received 1 June 2002; published 16 July 2003)

We report on the experimental realization of an atom optical device that allows scanning of an atomic beam with a controllable diffraction grating for atomic waves. We used a time-modulated evanescent wave field above a glass surface to diffract a continuous beam of metastable neon atoms at grazing incidence. The diffraction angles and efficiencies were controlled by the frequency and form of modulation, respectively. With an optimized shape, obtained from a numerical simulation, we were able to transfer more than 50% of the atoms into the first order beam, which we were able to move over a range of 8 mrad.

DOI: 10.1103/PhysRevA.68.013606

PACS number(s): 03.75.-b, 32.80.Pj, 42.50.Vk

Advances in optical manipulation of neutral atoms have brought developments in atom lithography, the process of creating an arbitrary pattern on a solid surface. Nanometer scale patterns were produced using a standing wave of light placed in the proximity of the surface [1–3]. More recently, an arbitrary pattern was drawn from a distance holographically [4], using quantum reflection from a surface microstructure. Previously, the creation of arbitrary patterns was achieved with thin-film transparent holograms [5–8].

A different approach to creating arbitrary patterns is to scan an atomic beam combined with an atomic focusing lens, which can be realized using electrostatic [9], magnetic [10], or microwave fields [11], or a thin-film Fresnel-zone plate [12]. The intensity pattern can then be written on a surface, in analogy to electron beam lithography.

We report in this article on the experimental realization of an atomic-wave scanner, which makes it possible to control the position of an atomic beam by an electronic signal. We diffracted a metastable atomic beam at grazing incidence from a glass surface by using a time-modulated evanescent wave. Our technique was the spatial version of the work by Steane *et al.* [13] and by Szriftgiser *et al.* [14], in which they generated frequency sidebands of nhf with a sinusoidally modulated evanescent light of frequency f in a perpendicularly reflected atomic beam. Diffraction of matter waves from vibrating mirrors has also been performed with neutrons [15].

Diffraction of an atomic beam has been proposed and demonstrated by using a free standing optical wave [16], a standing evanescent wave [17–19], and an evanescent wave on a periodically structured glass surface [20]. To change the angle of the diffracted atoms in this scheme, one has to rotate the prism or mirror mechanically. If a time modulation is added to the interaction potential, the angle can be varied electronically by changing the modulation frequency. This technique has been used in the standing optical wave case [21–23]. Furthermore, the diffracted atoms can be concentrated into a single order by properly tailoring the modulation wave form.

Due to the averaging of the periodic light potential modulation along the trajectory of the atom, it is difficult to obtain

efficient diffraction into nonzero orders, if the atom does not pass through the interaction region within a period of modulation $1/f$. Since the thickness of the evanescent field is on the order of the optical wavelength, this condition can be easily satisfied, and we obtained diffraction into a single order with an efficiency of more than 50%.

Modulation of the potentials in time leads to the absorption of energy quanta, which by analogy has been called “diffraction in time.” In our configuration, the absorption of energy quanta perpendicular to the surface leads to a splitting of the atomic beam into diffraction orders, that are separated in space. Since there is no gradient parallel to the mirror plane, the momentum parallel to the surface does not change. The diffraction angles are then readily calculated:

$$\Theta_{o,n} = \sqrt{\Theta_i^2 + n \frac{hf}{mv^2/2}}, \quad n=0, \pm 1, \pm 2, \dots \quad (1)$$

Here Θ_i and $\Theta_{o,n}$ denote the angles of incidence and diffraction of order n , respectively, f is the modulation frequency, v is the incident velocity, and m is the atomic mass.

Figure 1 shows our experimental setup. Metastable neon atoms in the $1s_5[{}^3P_2]$ state were first trapped and cooled in a magneto-optical trap (MOT) [24] using a four-beam configuration [25]. By focusing a 598 nm laser into the cloud of

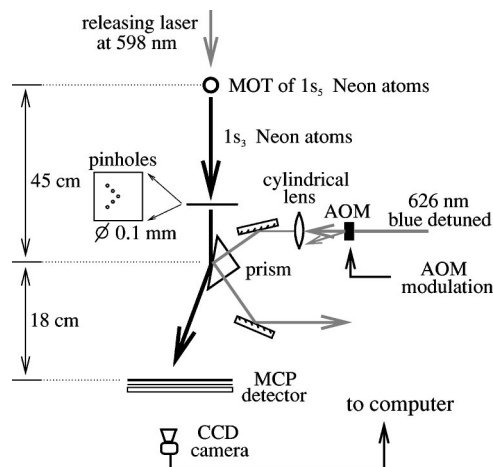


FIG. 1. Experimental setup.

*Electronic address: hilmar@ils.uec.ac.jp

trapped atoms, we optically pumped about half of the atoms to the $1s_3[{}^3P_0]$ state, which caused them to start a free fall pulled by gravity. The other half decayed to the ground state by emitting a 74 nm ultraviolet photon. An additional laser, red detuned with respect to the transition at 626 nm, was overlapped with the 598 nm laser and focused onto the trap. The 626 nm laser formed an attractive dipole potential around the trap, which increased the flux and reduced the momentum spread of the atomic beam. The setup of the source and MOT was similar to that described in [5,6,26]. All lasers were continuous wave, single frequency dye lasers.

The atoms illuminated a mask with five pinholes of 0.1 mm diameter. The atoms passing through the central hole, which was aligned exactly below the trap, were reflected by the evanescent wave mirror, placed 6 cm below the mask. The angle of incidence was around 21 mrad. Atoms that passed through the four off-axis pinholes were used for the calibration of the beam intensity.

The atom mirror was realized by total internal reflection of an intense, blue detuned laser beam in a BK7 glass prism. We used the optical dipole potential originating from the transition at 626 nm and worked with a detuning of about +2 GHz. The laser beam passed through an acousto-optical modulator (AOM), and by modulating the rf intensity of the AOM driver, we created the desired light intensity modulations. The average laser power was between 100 and 150 mW. The beam had an elliptical Gaussian shape with $1/e^2$ diameters of 7×0.8 mm at the prism. The beam diameters were chosen to be slightly larger than the size of the pinhole in order to be able to neglect the influence of the beam shape in our optimization procedure.

The prism was placed 45 cm from the trap center, corresponding to an atomic velocity of 3 m s^{-1} . The velocity dispersion, which we were able to estimate from the number of atoms transmitted through the off-axis pinholes, was compressed due to the acceleration in the gravitational field and amounted to about 1% of the vertical velocity. The width of the atomic beam is determined by the size of the pinholes.

The atoms were detected by a microchannel-plate detector (MCP) placed 63 cm from the trap. The MCP fluorescence plate was imaged onto a charge-coupled device (CCD) camera, equipped with an image intensifier. The signal was registered on commercial video tape, which was run later to retrieve the data with a computer. This setup allowed us to determine the position of each single atom incident on the detector.

Since the ultraviolet photons emitted from the trap were also detected by the MCP, we periodically switched the electric discharge of the neon source, MOT trapping beams, and the 598 nm releasing laser on and off. The period of this switching was 0.8 s, corresponding to about twice the time of free fall between the trap and the MCP. We recorded only atoms that arrived at the MCP when the MOT was off. On average, about 20 atoms were detected by the MCP per second.

Typical outputs from the MCP plate are shown in Figs. 2(a) and 2(b). The spot size of the diffracted beams was

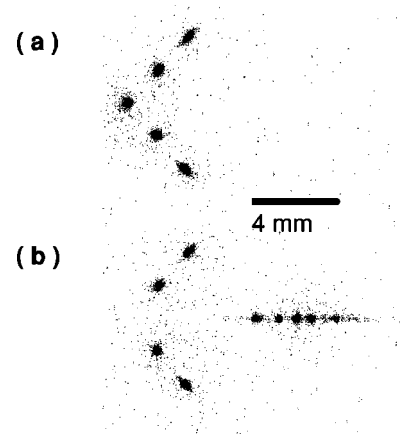


FIG. 2. Example output from the CCD camera. The intensity of each spot is not to scale. (a) Pattern of atoms on the MCP without the atom mirror. The mask pattern is imaged on the MCP. (b) The atoms passing through the central pinhole are diffracted by the modulated mirror.

approximately the same as that of the incident beam, showing that beam divergence was not increased during diffraction.

In order to calculate the diffraction pattern we solved the one-dimensional, time-dependent Schrödinger equation, describing the reflection of a Gaussian wave packet, incident with velocity $v_{\perp} = v \Theta_i$, from the time-modulated potential. It is not necessary to solve the two-dimensional equation, since the relative intensity of the diffraction orders is insensitive to the propagation parallel to the mirror surface.

The equation was solved numerically using the algorithm described in [27], Chapter 19.2. In this calculation we also included the van der Waals surface potential, taking the result from [26]:

$$V(t, z) = V_0(t) e^{-2\kappa z} - \frac{C_4}{(z + \lambda/2\pi)z^3} \quad (2)$$

with $C_4 = 7.3 \times 10^{-56} \text{ J m}^4$ and $\lambda = 5.0 \text{ } \mu\text{m}$. We set the potential to zero in the region where it would be negative, in order to avoid the singularity at $z=0$. The van der Waals potential reduces the height of the evanescent-wave potential barrier by approximately a factor of 2 and modifies the shape of modulation. Also, if the minimum of $V(t, z)$ is lower than the incident energy, some fraction of the atoms passes the potential barrier and is lost.

We optimized the shape of modulation in order to transfer a maximum amount of atoms into one of the first order beams. The arbitrary shape of the modulation of the optical light potential was described by a Fourier series:

$$V_0(t) = V_0 \left[1 + \epsilon \sum_{n=1}^N c_n \sin(n2\pi ft + \phi_n) \right], \quad (3)$$

and eight harmonics were included in the simulation ($N = 8$). The optimum amplitudes c_n , phases ϕ_n , and modulation depth ϵ were then determined by fitting the calculated diffraction efficiencies to the chosen ideal distribution:

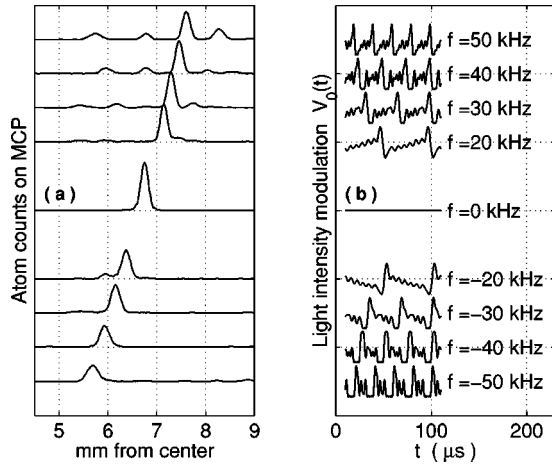


FIG. 3. (a) The relative intensity of diffracted atoms when the wave form was optimized to concentrate atoms into a single diffraction order. (b) The wave form for each modulation frequency in (a). For better visibility, the experimental data have been filtered with a second order Savitzky-Golay filter [27] in this picture.

$|a_1|^2 = 1$ or $|a_{-1}|^2 = 1$ and all other $|a_k|^2$ zero, where $|a_k|^2$ is the relative intensity of the k th diffraction order. The procedure was repeated for each modulation frequency f , and the optimum values also depended on other experimental parameters, such as the potential height or the angle of incidence of the laser beam on the prism. The result of these calculations is shown in Fig. 3(b) for a frequency range between -50 and $+50$ kHz. The negative frequency axis corresponds to the negative first order and the positive axis to the positive first order. Full modulation ($\epsilon = 1$) was found to be always optimum for our parameter range.

Figure 3(a) shows the measured distributions of atoms on the MCP obtained by modulating the laser intensity with the optimized forms. The strong peak is the first diffraction order.

Our results are summarized in Fig. 4. Figure 4(a) shows the measured and calculated reflectivities, i.e., the number of all coherently diffracted atoms divided by the number of all atoms incident on the mirror, as a function of the modulation frequency. The reflectivity was obtained by counting the atoms in the diffracted peaks and the atoms transmitted through the central pinhole when the mirror was removed. We used the number of atoms falling through the four off-axis pinholes to scale the intensity. The reflectivity was near 100% on the positive frequency axis, but decreased slightly on the negative frequency axis with higher frequencies. This is because the fraction of time in which the height of the potential was lower than the incident energy of the atoms was increasing along with the frequency.

Figure 4(b) shows the measured and calculated relative diffraction efficiencies and 4(c) the diffraction angles for the optimized shapes. The values obtained with a sawtooth shaped modulation (modulation depth $\epsilon = 0.5$) are plotted for comparison. The relative diffraction efficiency, i.e., the intensity of the first order peak divided by the total intensity of all peaks, was determined in the following way. We first summed all points perpendicular to the plane of reflection.

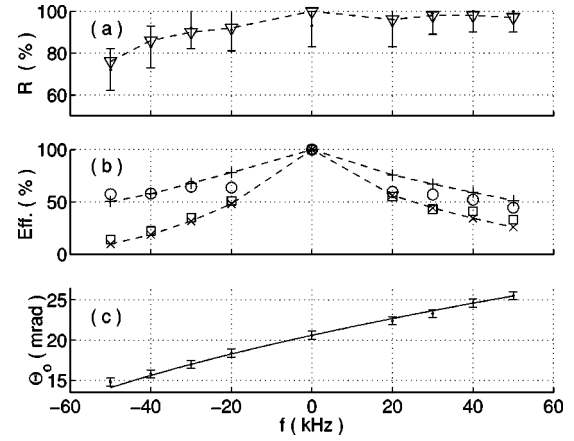


FIG. 4. (a) Measured (error bars) and calculated (∇) reflectivities. (b) Measured (\circ) and calculated ($+$) relative efficiencies using the optimized shapes. For comparison the values obtained with a sawtooth shaped modulation are shown ($\epsilon = 0.5$; \square , measured and \times , calculated). The values for negative first order are plotted on the negative, and the values for positive first order on the positive frequency axis. The marker size corresponds to the uncertainties. (c) Diffraction angle (Θ_0) vs modulation frequency. The solid line shows the predicted values calculated with Eq. (1). All uncertainties were estimated from the statistical fluctuations of repeated measurements. Calculated points have been joined by dashed lines for better visibility.

The distribution of atom counts was then fitted by a sum of Gaussians, which allowed us to determine the intensity and position of each peak. For modulation frequencies smaller than approximately 20 kHz, however, the peaks of different diffraction orders overlapped, and their intensities could not be accurately determined.

The agreement of experimental data with calculated values is reasonable, although the measured efficiencies were slightly less than expected for the optimized shapes. This discrepancy may be due to small differences between the actual experimental parameters and the values assumed in the calculation of the curves, or to the spatial variation of the evanescent wave light.

Nevertheless, we were able to scan the atomic beam, which contained more than 50% of the incident atoms, in a range of about 8 mrad. Fewer than 10% of the incident atoms were left in the zeroth order beam over the whole range.

The frequency range, and hence the scanning range, could be further extended by reducing the interaction time of the atoms with the mirror. This could be achieved by using a prism with higher refractive index, larger angle of incidence of the laser beam on the prism, or higher incident velocity of the atoms.

In conclusion, we have demonstrated the manipulation of an atomic beam with a time-modulated evanescent wave mirror. With an optimized shape of modulation, which can be determined from a numerical solution of the time-dependent, one-dimensional Schrödinger equation, the majority of atoms can be transferred into only one diffraction order. Extended to two dimensions and combined with a focusing device, the present technique might be applied in atom lithography to write a pattern onto a surface, as well as to realize a scanning

microscope of neutral atoms to investigate surface characteristics. Focusing of the atomic beam should be possible by using a curved mirror. The same method could also be used to realize a 50/50 beam splitter or to couple atoms into an atomic cavity [28].

The authors would like to thank M. Morinaga, A. Suzuki, and J. Lodewyck for their help in the experiment. This work was partly supported by Grant in Aid for Scientific Research (No. 11216202) from the Ministry of Education, Culture, Sports, Science and Technology, Japan.

-
- [1] A. Bell *et al.*, Surf. Sci. **433-435**, 40 (1999), and references therein.
- [2] J. Thywissen *et al.*, J. Vac. Sci. Technol. B **15**, 2093 (1997).
- [3] M. Mutzel *et al.*, Phys. Rev. Lett. **88**, 083601 (2002).
- [4] F. Shimizu and J. Fujita, Phys. Rev. Lett. **88**, 123201 (2002).
- [5] J. Fujita *et al.*, Nature (London) **380**, 691 (1996).
- [6] M. Morinaga, M. Yasuda, T. Kishimoto, and F. Shimizu, Phys. Rev. Lett. **77**, 802 (1996).
- [7] J. Fujita, S. Mitake, and F. Shimizu, Phys. Rev. Lett. **84**, 4027 (2000).
- [8] T. Kishimoto, J. Fujita, S. Mitake, and F. Shimizu, Jpn. J. Appl. Phys., Part 1 **38**, 683 (1999).
- [9] H. Noh, K. Shimizu, and F. Shimizu, Phys. Rev. A **61**, 041601(R) (2000).
- [10] W. Kaenders, Phys. Rev. A **54**, 5067 (1996).
- [11] K. Shimizu *et al.*, in *Laser Spectroscopy, XII International Conference*, edited by M. Inguscio, M. Allegrini, and A. Sasso (World Scientific, Singapore, 1996), p. 140.
- [12] O. Carnal *et al.*, Phys. Rev. Lett. **67**, 3231 (1991).
- [13] A. Steane, P. Szriftgiser, P. Desbiolles, and J. Dalibard, Phys. Rev. Lett. **74**, 4972 (1995).
- [14] P. Szriftgiser, D. Guéry-Odelin, M. Arndt, and J. Dalibard, Phys. Rev. Lett. **77**, 4 (1996).
- [15] J. Felber *et al.*, Phys. Rev. A **53**, 53 (1996).
- [16] P. Martin, B. Oldaker, A. Miklich, and D. Pritchard, Phys. Rev. Lett. **60**, 515 (1988).
- [17] J. Hajnal and G. Opat, Opt. Commun. **71**, 119 (1989).
- [18] M. Christ *et al.*, Opt. Commun. **107**, 211 (1994).
- [19] C. Henkel *et al.*, Appl. Phys. B: Lasers Opt. **69**, 277 (1999), and references therein.
- [20] V. Balykin, D. Lapshin, M. Subbotin, and V. Letokhov, Opt. Commun. **145**, 322 (1998).
- [21] S. Bernet *et al.*, Phys. Rev. A **62**, 023606 (2000), and references therein.
- [22] S. Bernet *et al.*, J. Opt. Soc. Am. B **15**, 2817 (1998).
- [23] S. Bernet *et al.*, Proc. R. Soc. London, Ser. A **455**, 1509 (1999).
- [24] E. Raab *et al.*, Phys. Rev. Lett. **59**, 2631 (1987).
- [25] F. Shimizu, K. Shimizu, and H. Takuma, Opt. Lett. **16**, 339 (1991).
- [26] F. Shimizu, Phys. Rev. Lett. **86**, 987 (2001).
- [27] W. Press, B. Flannery, S. Teukolsky, and W. Vetterling, *Numerical Recipes in C: The Art of Scientific Computing*, 2nd ed. (Cambridge University Press, Cambridge, 1992).
- [28] V. Balykin and V. Letokhov, Appl. Phys. B: Photophys. Laser Chem. **48**, 517 (1989).